International Journal of Applied Mathematics

Volume 32 No. 1 2019, 141-154
ISSN: 1311-1728 (printed version); ISSN: 1314-8060 (on-line version)
doi: http://dx.doi.org/10.12732/ijam.v32i1.13

NEW BOUNDARY CONDITION FOR THE TWO DIMENSIONAL STATIONARY BOUSSINESQ PARADIGM EQUATION

Krassimir Angelow

Institute of Mathematics and Informatics
Bulgarian Academy of Sciences, Acad. G. Bonchev Str., Block 8
Sofia – 1113, BULGARIA

Abstract: The paper considers stationary propagating wave solutions to a two dimensional Boussinesq equation. It is nonlinear, fourth order, elliptic equation. A new boundary condition (BC) on the computational boundary is proposed and applied. The numerical algorithm for computation of stationary propagating waves is based on high order accurate finite difference schemes. The performed numerical tests confirm the validity of the new BC. A comparison with the known in the literature formulas is also given.

AMS Subject Classification: 37K40, 37L50, 65M06
Key Words: stationary wave, two dimensional Boussinesq equation, boundary, soliton, uniform grid, false transient method

Received: January 12, 2019

1. Introduction

function notation	function arguments	explanation
u	x, y, t	analytical solution for the hyperbolic equation (1), (2)
U	x, y, r	analytical solution for the elliptic equation (3)
$\bar{v}$	$\bar{x}, \bar{y}, \bar{r}$	analytical solution for the Laplace equation (8) (Section 3 only)
$\tilde{U}, \tilde{W}$	$\tilde{x}, \tilde{y}, \tilde{r}$	analytical solution for the elliptic system (15) after variable change (14)
$\widehat{U}, \widehat{W}$	$\tilde{x}, \tilde{y}, \tilde{r}$	analytical solution for the elliptic system (16), (17) after fixing $\widehat{U} = \tilde{U}/\theta$

2. Introduction

In this paper we consider stationary solutions (solutions of type $u(x, y, t) = U(x, y - ct)$) to the two dimensional Boussinesq Paradigm Equation (BE)

$$u_{tt} - \Delta u - \beta_1 \Delta u_{tt} + \beta_2 \Delta^2 u + \Delta f(u) = 0 \text{ for } (x, y) \in R^2,\ t \in R^+, \tag{1}$$

$$\begin{aligned} &u(x, y, 0) = u_0(x, y),\ u_t(x, y, 0) = u_1(x, y) \quad \text{for} \quad (x, y) \in R^2, \\ &u(x, y) \to 0, \Delta u(x, y) \to 0, \quad \text{for} \quad \sqrt{x^2 + y^2} \to \infty, \end{aligned} \tag{2}$$

where $f(u) = \alpha u^2$, $\alpha > 0$, $\beta_1 > 0$, $\beta_2 > 0$ are dispersion parameters, and Δ is the Laplace operator.

A derivation of the BE from the original Boussinesq system with discussion on the different mechanical properties could be found e.g. in [1].

The one-dimensional (1D) BE is famous with its approximation for long waves propagating in shallow water [2, 3]. Furthermore, 1D BE admits localized wave solutions (called solitons),

$$u_{tt} - u_{xx} - \beta_1 u_{xxtt} + \beta_2 u_{xxxx} + f(u)_{xx} = 0,$$

which maintain shape and emerge unchanged from collisions with other traveling waves, appear to be a very suitable model for particles [4, 5]. Let us find a stationary, traveling in y direction with phase velocity c, wave solution to the 2D BE, i.e. a solution to (1), (2) of type $u(x, y, t) = U(x, y - ct)$. The waves U satisfy the nonlinear fourth order elliptic equation:

$$c^2(E - \beta_1\Delta)U_{yy} = \Delta U - \beta_2\Delta^2 U - \Delta f(U), \quad (3)$$

where E is the identity operator. If the condition $c < \min(1/\sqrt{\beta}, 1)$, with $\beta = \beta_1/\beta_2$ holds, then (3) is an elliptic equation of fourth order and the linear second order derivatives in (3) form a second order elliptic equation. Only velocities c which fulfill this inequality are considered.

The main goal is to evaluate numerically the stationary solitary waves U to (1), which are solutions to (3). In the future, it is planned to investigate such waves as potential 2D soliton-like candidates for the nonstationary equation (1). This includes but is not limited to evolution in time of the resultant shape and collision of two surges.

Different techniques have been applied through the investigation of the elliptic problem (3). The false transient method and the galerkin spectral method are used in [6, 8]; the Fourier Galerkin method is implemented in [7, 8] and the “perturbation solution - in [9]. We emphasize that both problems, Eq. (1) and Eq. (3), are posed on unbounded domain the plane R^2. Thus we have to numerically limit the computational domain so that the results could approximate the exact solution for the unbounded domain and, moreover, to keep the overall computational cost reasonable. Thus an artificial boundary Ω and artificial boundary conditions (BC) are stated, known in the literature as absorbing BC or nonreflecting BC (see [10] for a wave equation, [11] for a Helmholtz type equation, [12] for elliptic second order equation, etc.).

The problem for posing artificial BC for BE is studied in [6], where the following asymptotics of U is found

$$U(x, y) = U(r) \sim C_u/r^2, \quad \text{for} \quad r >> 1, \quad (4)$$

for sufficiently large $r = \sqrt{x^2 + y^2}$. In this paper a new and more sophisticated artificial BC for stationary BE (3)

$$U(r) = \mu\frac{(1 - c^2)x^2 - y^2}{(1 - c^2)x^2 + y^2}, \quad r >> 1 \quad (5)$$

is proposed. The condition (5) has an analytical form, which directly depends on x, y and the velocity c. Furthermore, high order finite difference schemes are used for numerical evaluation of the solution to problem (3). The new BC (5) and the numerical method are validated by performing a series of experiments, as mesh refinement and computations on different space domains. A comparison of the obtained here results with the similar results from [9] is also discussed.

3. Derivation of the new asymptotic boundary conditions

Problem (3) can be rewritten as a system of two elliptic equations of second order in different ways. We expect that the derivative U_{xx} in x direction will be smaller than the derivative U_{yy} in y direction because the solution moves along the y-axis. Therefore the equality $U_{yy} = \Delta U - U_{xx}$ is substituted in (3) and after introducing an auxiliary function W, we obtain an equivalent to (3) system of two elliptic equations:

$$\begin{aligned} &(1-c^2)U + (c^2\beta_1 - \beta_2)\Delta U - f(U) = W, \\ &-\Delta W = c^2(E - \beta_1\Delta)U_{xx}. \end{aligned} \tag{6}$$

We have to complete the system (6) with appropriate boundary conditions for functions U and W. In [6] the behavior of the solution $U(r)$ for $r = \sqrt{x^2+y^2} \to \infty$ is studied in details. From the mathematical analysis and numerical results provided there it follows that U(r) and W(r) have $O(r^{-2})$ asymptotic decay at infinity.

Let us go further and estimate which terms in the equations (3), define the asymptotic behavior of the solution. At first, suppose that for sufficiently large r the second order derivatives $\Delta U, c^2U_{xx}$, c^2U_{yy} of U are of order $O(r^{-4})$, whereas the fourth order derivatives and the nonlinear term, i.e. $\Delta^2 U, c^2\Delta U_{xx}$, $c^2\Delta U_{yy}$, $\Delta f(U)$ in equation (3) are of order $O(r^{-6})$. Now consider equation (3) for sufficiently large values of r. We insert the asymptotic values of all terms in (3) and neglect the higher order terms of order $O(r^{-6})$ inside the r-expansion. Thus for large values of r the following formulas are valid:

$$\Delta\bar{U}(x,y) = c^2\bar{U}_{yy}(x,y), \;\; \bar{U}(x,y) \sim \frac{1}{x^2+y^2} \;\text{ for }\; x^2+y^2 \to \infty. \tag{7}$$

We apply the following change of variables

$$\bar{x} = \sqrt{1-c^2}x, \quad \bar{y} = y, \quad \bar{v}(\bar{x},\bar{y}) := \bar{U}(x,y)$$

and transform (7) into the Laplace equation for the new function $\bar{v}$,

$$\Delta\bar{v} = 0, \quad \bar{v}(\bar{x},\bar{y}) \sim \frac{1}{\bar{r}^2}, \quad |\bar{r}| = \sqrt{\bar{x}^2+\bar{y}^2} \to \infty. \tag{8}$$

In polar coordinates the Laplace equation (8) is rewritten as:

$$\frac{\partial^2}{\partial \bar{r}^2}\bar{v}(\bar{r},\psi) + \frac{1}{\bar{r}}\frac{\partial}{\partial \bar{r}}\bar{v}(\bar{r},\psi) + \frac{1}{\bar{r}^2}\frac{\partial^2}{\partial \psi^2}\bar{v}(\bar{r},\psi) = 0. \tag{9}$$

After the separation of variables $\bar{v}(\bar{r},\psi) = H(\bar{r})G(\psi)$ we get the following general form of functions G and H:

$$H(\bar{r}) = \sum_{n=0}^{\infty}(\mu_{1,n}\frac{1}{\bar{r}^n} + \mu_{2,n}\bar{r}^n), \tag{10}$$

$$G(\psi) = \sum_{n=0}^{\infty}(\mu_{3,n}\sin(n\psi) + \mu_{4,n}\cos(n\psi)).$$

By following the asymptotic limitation that $H(\bar{r}) \sim \frac{1}{\bar{r}^2}$ for $|\bar{r}| \to \infty$ all parameters $\mu_{1,n}, n \neq 2$ and $\mu_{2,n}, n \geq 0$ are set to zero and thus $H(\bar{r}) = \mu_{1,2}\frac{1}{\bar{r}^2}$. Similar simplification is made for the second function G. It is known that the x and y axis on the plane are lines of symmetry for the soliton solution. In order to fit this symmetrical behaviour, all parameters $\mu_{3,n}, \mu_{4,n} n \neq 2$ are set to zero. For directness and clarity the term $\mu_{3,2}\sin(2\psi)$ is also neglected and thus $H(\psi) = \mu_{4,2}\cos(2\psi)$. In this way the following representation of the main asymptotic term $\bar{v}$ of the solution is obtained:

$$\bar{v}(\bar{r}\psi) = \mu_u\frac{\cos(2\psi)}{\bar{r}^2} = \mu_u\frac{\cos(\psi)^2 - \sin(\psi)^2}{\bar{r}^2} = \mu_u\frac{\bar{x}^2 - \bar{y}^2}{(\bar{x}^2 + \bar{y}^2)^2}, \tag{11}$$

where $\mu_u = \mu_{1,2}\mu_{4,2}$. In the old (x, y) coordinate system, (11) reads as:

$$U(x,y) = \mu_u\frac{(1-c^2)x^2 - y^2}{((1-c^2)x^2 + y^2)^2}. \tag{12}$$

We treat the second function W from (6) in a similar way and obtain analogous asymptotic representation:

$$W(x,y) = \mu_w\frac{(1-c^2)x^2 - y^2}{((1-c^2)x^2 + y^2)^2}. \tag{13}$$

The proposed formulas (12) and (13) are used as candidates for a BC and series of numerical tests are done to prove their validity in Section 5. It is expected that by increasing the size of the domain Ω, the numerical solution near boundary converges faster, and the μ_u and μ_w parameters settle down (see Test 1). It is also expected that the numerical solution behaves asymptotically as $\frac{1}{r^2}$ for larger $r >> 1$ (see Test 2). The parameters μ_u and μ_w are found in a procedure described in Section 4.3.

4. Numerical method for the elliptic system

4.1. Formulation

In order to relate to our previous results from [13, 14], we make the following change of variables

$$\begin{aligned} &x = \sqrt{\beta_1}\tilde{x}, y = \sqrt{\beta_1}\tilde{y}, \\ &U(x,y) = \tilde{U}(\tilde{x},\tilde{y}), \frac{\beta_1}{\beta_2}W(x,y) = \tilde{W}(\tilde{x},\tilde{y}). \end{aligned} \tag{14}$$

Thus, the system (6) is transformed into new elliptic system:

$$\begin{aligned} &(\beta - \tilde{c}^2)\tilde{U} - (1-\tilde{c}^2)\Delta\tilde{U} - \beta f(\tilde{U}) = \tilde{W}, \\ &-\Delta\tilde{W} = \tilde{c}^2(E-\Delta)\tilde{U}_{\tilde{x}\tilde{x}}, \end{aligned} \tag{15}$$

with $\beta = \beta_1/\beta_2$ and $\tilde{c} = \sqrt{\beta}c$.

We seek non-trivial solutions to (15). To avoid the trivial solution we proceed as in [6]: the value of the solution $\tilde{U}$ at the point $(0,0)$ is fixed, $\tilde{U}(0,0) = \theta$, and new functions are introduced: $\widehat{U} = \tilde{U}/\theta$ and $\widehat{W} = \tilde{W}/\theta$. Thus $\widehat{U}(0,0) = 1$ and from (15) we get

$$\begin{aligned} &(\beta - \tilde{c}^2)\widehat{U} - (1-\tilde{c}^2)\Delta\widehat{U} - \alpha\beta\theta\widehat{U}^2 = \widehat{W}, \\ &-\Delta\widehat{W} = \tilde{c}^2(E-\Delta)\widehat{U}_{\tilde{x}\tilde{x}}. \end{aligned} \tag{16}$$

The value of θ is found from the equation

$$\theta = \frac{(1-\tilde{c}^2)\Delta\widehat{U} - (\beta-\tilde{c}^2)\widehat{U} + \widehat{W}}{\alpha\beta\widehat{U}^2}\Big|_{\tilde{x}=0,\tilde{y}=0}. \tag{17}$$

In order to evaluate numerically the solution to (16) artificial time is introduced, false time derivatives are added and one gets

$$\begin{aligned} &\frac{\partial\widehat{U}}{\partial t} + (\beta - \tilde{c}^2)\widehat{U} - (1-\tilde{c}^2)\Delta\widehat{U} - \alpha\beta\theta\widehat{U}^2 = \widehat{W}, \\ &\frac{\partial\widehat{W}}{\partial t} - \Delta\widehat{W} = \tilde{c}^2(E-\Delta)\widehat{U}_{\tilde{x}\tilde{x}}. \end{aligned} \tag{18}$$

Thus the solution to the steady coupled elliptic system (16) is replaced by solving the pertinent transient equations (18) until their solutions $\widehat{U}$ and $\widehat{W}$ cease to change significantly in time.

4.2. Discretization

The unbounded domain R^2 is replaced by a sufficiently large computational domain Ω. Due to the obvious symmetry of the problem, we can look for the solution only in the first quadrant $\Omega = [0, L_x] \times [0, L_y]$.

The uniform and non-uniform grid define two different investigation approaches to discretization of (18) in Ω. The meshing, that has been predominantly used in most cited papers for the numerical analysis of BE, is the non-uniform one, see e.g. [6]. It has big time advantage of generating a fast solution for the system (18), but also creates a major problem when using the solution of (18) as initial data for hyperbolic equation (1). The ultimate goal is to develop an algorithm which investigates collision of two waves with arbitrary phase speeds $\tilde{c}$. Shifting the traveling waves in the hyperbolic equation on a larger distance, and further colliding two 'soliton-like' solutions requires a uniform grid. Therefore we decide to apply a uniform grid to solve equation (3) ((18) respectively). A uniform grid Ω_h is defined in the following way:

$$\Omega_h = \{(\tilde{x}_i, \tilde{y}_j) : \tilde{x}_i = ih, \tilde{y}_j = jh, i = 0, \cdots, N_x, j = 0, \cdots, N_y\},$$

where the discretization step h satisfies $h = L_x/N_x = L_y/N_y$.

The value of the function $\widehat{U}$ at mesh point $\tilde{x}_i, \tilde{y}_j, t_k$ is denoted by $\widehat{U}^k_{i,j}$.

The spatial derivatives in (18) are defined by using centered finite differences and extending the stencil:

$$\widehat{U}_{\tilde{x}\tilde{x},p}(\tilde{x}) := \frac{1}{h^2} \sum_{i=-p/2}^{p/2} d_i \widehat{U}(\tilde{x} + ih), \tag{19}$$

Here p is equal to 2, 4 or 6. The weights d_i taken from [16] are $1, -2, 1$ for $p = 2$, $-\frac{1}{12}, \frac{4}{3}, -\frac{5}{2}, \frac{4}{3}, -\frac{1}{12}$ - for $p = 4$ and $\frac{1}{90}, -\frac{3}{20}, \frac{3}{2}, -\frac{49}{18}, \frac{3}{2}, -\frac{3}{20}, \frac{1}{90}$ - for $p = 6$. The approximation error of formulae (19) is $O(h^p)$. Replacing the Laplace operator in (18) by the discrete Laplacian

$$\Delta_{h,p}\widehat{U}_{i,j} := (\widehat{U}_{i,j})_{\tilde{x}\tilde{x},p} + (\widehat{U}_{i,j})_{\tilde{y}\tilde{y},p},$$

we obtain finite difference schemes with high order of approximation $O(h^4)$ for $p = 4$ and $O(h^6)$ for $p = 6$. The application of FDS with high order of approximation leads to a high rate of convergence of the method when solutions are sufficiently smooth. In this way more accurate numerical solutions can be produced on a coarse grid.

Symmetry conditions are used to impose the values of the discrete Laplacian at mesh points close to lines $\{(0, y) : y < L_y\}$, and $\{(x, 0) : x < L_x\}$. Near the computational boundaries $\{(L_x, y) : y < L_y\}$ and $(x, L_y) : x < L_x\}$ we do not change the stencil. The discrete Laplacian is defined there by using the values of the discrete solution given in (12) and (13) at points outside the computational domain.

4.3. Numerical Method

The Euler explicit rule is applied for approximation of time derivatives. The nonlinear terms in (18) are computed on time level t^k. Thus, the numerical solutions at time level t^{k+1} are evaluated directly by the values of the numerical solution at time level t^k:

$$\begin{aligned} &\frac{\widehat{U}^{k+1}_{i,j} - \widehat{U}^{k}_{i,j}}{\tau} - (1-\tilde{c}^2)\Delta_{h,p}\widehat{U}^{k}_{i,j} + (\beta - \tilde{c}^2)\widehat{U}^{k}_{i,j} - \alpha\beta\theta(\widehat{U}^{k}_{i,j})^2 = \widehat{W}^{k}_{i,j}, \\ &\frac{\widehat{W}^{k+1}_{i,j} - \widehat{W}^{k}_{i,j}}{\tau} - \Delta_{h,p}\widehat{W}^{k}_{i,j} = \tilde{c}^2(E - \Delta_{h,p})\widehat{U}^{k}_{i,j,\tilde{x}\tilde{x},p}. \end{aligned} \tag{20}$$

This method for solving equations (18) can be considered also as “the simple iteration method” for solving linear and nonlinear equations [15]. Last but not least, in order to start the procedure we need initial values for functions $\widehat{U}, \widehat{W}$. These initial values are taken from the formulae in [9].

The transformation (14) modifies the BC (12) and (13) in the following way:

$$\begin{aligned} &\widehat{U}_B(\tilde{x}, \tilde{y}) = \mu_u \widehat{B}(\tilde{x}, \tilde{y}), \quad \widehat{W}_B(\tilde{x}, \tilde{y}) = \mu_w \widehat{B}(\tilde{x}, \tilde{y}) \\ &\widehat{B}(\tilde{x}, \tilde{y}) = \frac{(1-\tilde{c}^2/\beta)\tilde{x}^2 - \tilde{y}^2}{((1-\tilde{c}^2/\beta)\tilde{x}^2 + \tilde{y}^2)^2}. \end{aligned} \tag{21}$$

In order to resolve the boundary functions in (21) completely, one needs the values of μ_u and μ_w. These are obtained iteratively, at each time level of the algorithm for solving problem (20), by the minimization procedure described below.

For a given numerical solution $\widehat{U}^k$ at the time level t_k we choose μ_u as minimizer of the problem

$$\mu_u = \min_{\mu_u > 0} ||\widehat{U}_B(\tilde{x}_i, \tilde{y}_j) - \widehat{U}^k_{i,j}||_{L_2, \Omega_B}, \tag{22}$$

where $(\tilde{x}_i, \tilde{y}_j) \in \Omega_B$. The set Ω_B includes not only the boundary nodes on $\partial\Omega_h$ but also inner nodes lying close (e.g. at distance $2h, 4h, 6h, ... << N_x h$) to the boundary. The minimization problem above (22) produces a simple linear equation with respect to μ_u.

5. Validation tests

Two tests are made to verify the new condition on the computational boundary where the finite difference schemes are fourth order of approximation and the following constants are fixed: $\alpha = 1, \beta = 3$ and $c = 0.45$.

5.1. Test 1.

It reviews the behavior of μ_u defined in (11) and numerically evaluated in (22). In Table 1, for computational domains $\tilde{\Omega}_h = [0, L_x] \times [0, L_y]$ with $L_x = L_y = 20, 40, 80, 160,$ and fixed domain discretiization step $h = 0.5$, the following quantities are presented at the end of the iteration procedure:

- values of the numerical solution $\widehat{U}_{i,j}$ at point: $\tilde{x}_i = 0$, $\tilde{y}_j = L_y$,
- values of μ_u,
- the L_2 norm of the error obtained in the minimization procedure (22).

$L_x = L_y$	$\widehat{U}^k_{i,j}$ at $\tilde{x}_i = 0$, $\tilde{y}_j = L_y$	μ_u	min $\|\|\widehat{U}_B(\tilde{x}_i, \tilde{y}_j) - \widehat{U}^k_{i,j}\|\|_{L_2,\Omega_B}$
20	-2.23e-04	1.9355e-01	4.17e-05
40	-5.65e-05	1.9369e-01	4.42e-06
80	-1.41e-05	1.9378e-01	7.56e-07
160	-3.53e-06	1.9381e-01	7.44e-10

Table 1: Characteristic parameters of the minimization procedure for different computational domains

The results in Table 1 demonstrate that the values of μ_u, shown in the third column, converge as the domain becomes larger. Further, the values of $\widehat{U}_{i,j}$ given in the second column decay with a rate of $\frac{1}{\tilde{r}^2}$ The results obtained for μ_w exhibit the same convergence, and are excluded for the sake of simplicity and compactness.

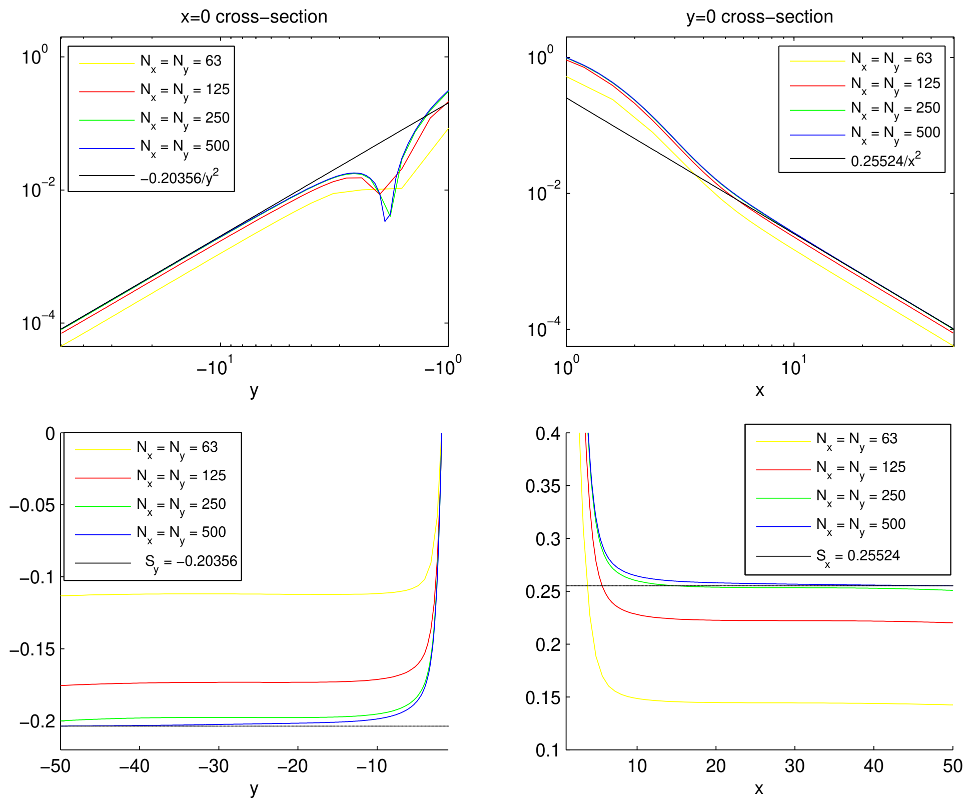

Figure 1: The effect of the mesh size. Upper pannels: funtion $\widehat{U}$ Lower panels: $\tilde{r}^2\widehat{U}$. $S_y = -\mu_u$, $S_x = \mu_u/(1-\tilde{c}^2/\beta)$, see (23).

5.2. Test 2.

The second test reveals the asymptotics of the numerical solution presented in log-log plots. Pictures in Figure 1 demonstrate important aspects of solution's cross sections on four different grids. The size of the computational domain is kept constant $\tilde{\Omega}_h = [0,50]\times[0,50]$, $c = \tilde{c}/\sqrt{\beta} = 0.45$ and only the discretization step changes, $h = 0.1, 0.2, 0.4, 0.8$.

The first two horizontal pictures in Figure 1 present logarithmic scaled plots of the absolute value of the numerical solution $\widehat{U}$. One can see the decay $\frac{1}{\tilde{r}^2}$ at infinity guided by the black line. The next two horizontal pictures show the numerical solution scaled by a factor $\tilde{r}^2$. Thus, these graphs display $\tilde{r}^2\widehat{U}$ along the vertical z axis. One can observe that the scaled profile of the solution approximates a constant for large values of $\tilde{r}$. These plots are in agreement with the new boundary function $\widehat{B}(\tilde{x}, \tilde{y})$ found in (21) and with the asymptotics of the solution. Further using formulae (21) for $\tilde{x} = 0$ or for $\tilde{y} = 0$ one has for sufficiently large $\tilde{r}$

$$\widehat{U}(0, \tilde{y}) = -\frac{\mu_u}{\tilde{y}^2}, \quad \widehat{U}(\tilde{x}, 0) = \frac{\mu_u}{(1 - \tilde{c}^2/\beta)\tilde{x}^2}. \tag{23}$$

The last equation explains the connection between the two constants (black line) displayed on botton pictures in Figure 1.

6. Results and Conclusion

On Figure 2, one could see the shape of the solution $\widehat{U}$ to problem (20) (equivalent to problem (3) in the reverse coordinate system (14)) for two combination of parameters $\tilde{c} = \sqrt{\beta}c$ and β: $c = 0.9, \beta = 1$ and $c = 0.5, \beta = 3$.

In this paper we evaluate the stationary propagating in direction y with speed c solutions to 2D BE. An iteration method is used to compute the solution of the corresponding fourth order nonlinear elliptic equation. A high order of approximation finite difference scheme is applied for the discretization of spatial derivatives.

A new BC is proposed on the boundary of the computational domain. Later the BC is verified by computation on different grids, using different speeds c and dispersion parameters β. Near the origin the form of the computed here stationary waves is similar to the presented in [9] form of 'best-fit' stationary solutions, but near the computational boundary both solutions are quite different.

The obtained analytical formulae (21) of the solution near the boundary give great advantage for the numerical computation of the solutions to the stationary BE (3) and (15) respectively. Instead of choosing bigger domain to represent the zero boundary conditions at infinity, one could use (21).

Results concerning convergence of the iterative method, shape of the solution, comparison of the numerical solution with the 'best-fit' formulae from [9] will be discussed in another article.

References

[1] C.I. Christov, An energy-consistent dispersive shallow-water model, *Wave Motion*, **34** (2001), 161-174.

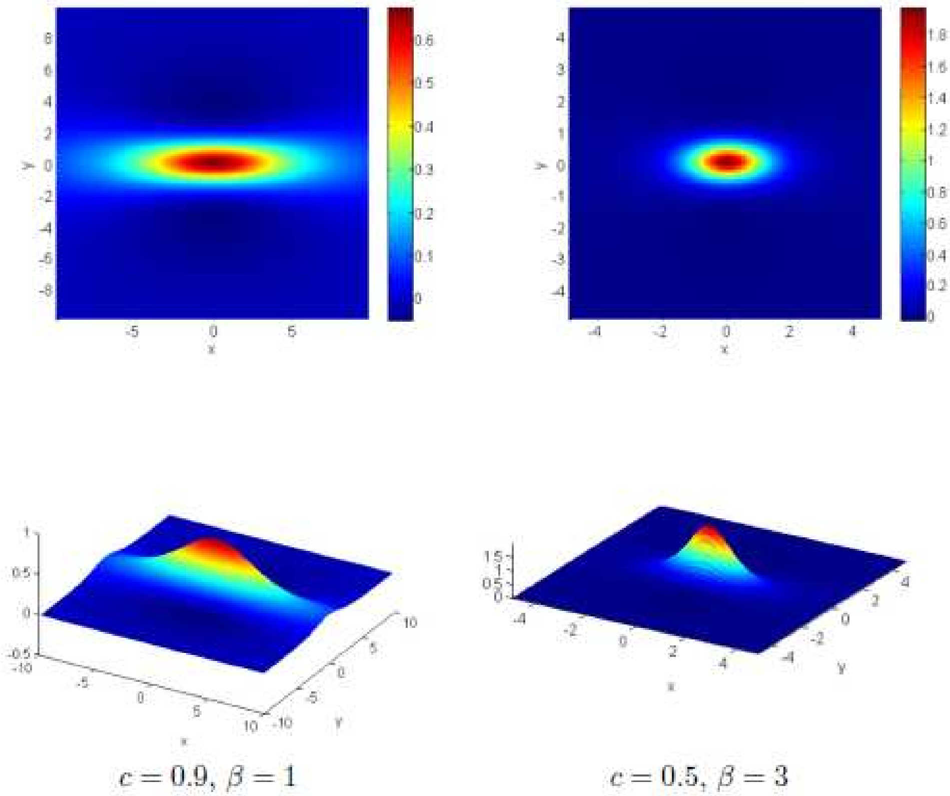

Figure 2: 2D and 3D solitonic shapes in a localized domain $[-10, 10] \times [-10, 10]$.

[2] J. Boussinesq, Theorie de lintumescence liquide, applelee onde solitaire ou de translation, se propageant dans un canal rectangulaire, *Comptes Rendus de lAcademie des Sciences* **72** (1871), 755-759.

[3] J. Boussinesq, Theorie des ondes et des remous qui se propagent le long dun canal rectangulaire horizontal, en communiquant au liquide contenu dans ce canal des vitesses sensiblement pareilles de la surface au fond, *Journal de Mathematiques Pures et Aplliquees, Deuxieme Serie*, **17** (1872), 55-108.

[4] I. Christov, C.I. Christov, Physical dynamics of quasi-particles in nonlinear wave equations, *Physics Letters A*, **372**, Issue 4 (2008), 841-848.

[5] J.K. Perring, T.H.R. Skyrme, A model unified field equation, *Nuclear Physics*, **31** (1962), 550-555.

[6] C.I. Christov, Numerical implementation of the asymptotic boundary conditions for steadily propagating 2D solitons of Boussinesq type equations, *Mathematics and Computers in Simulation*, **82** (2012), 1079-1092.

[7] M. Christou, C.I. Christov, Fourier Galerkin method for 2D solitons of Boussinesq equation, *Mathematics and Computers in Simulation* **74** (2007), 82-92.

[8] M. Christou, C.I. Christov, Galerkin spectral method for the 2D solitary waves of Boussinesq paradigm equation, In: *Applications of Mathematics in Technical and Natural Sciences, Sozopol (Bulgaria)*, *AIP Conference Proceedings*, **1186**, Issue 1 (2009), 217-225.

[9] C.I. Christov, J. Choudhury, Perturbation solution for the 2D Boussinesq equation, *Mech. Res. Commun.*, **38** (2011), 274-281.

[10] B. Engquist and A. Majda, Absorbing boundary conditions for the numerical simulation of waves, *Math. Comp.*, **31** (1977), 629651.

[11] C.I. Goldstein, A finite element method for solving Helmholtz type equations in waveguides and other unbounded domains, *Math. Comp.*, **39** (1982), 309324.

[12] H. Han, W. Bao, Error estimates for the finite element approximation of problems in unbounded domains, *SIAM J. Numer. Anal.* **37**, No 4 (2000), 11011119; DOI: 10.1137/S0036142998341805.

[13] N. Kolkovska, Two families of finite difference schemes for multidimensional Boussinesq paradigm equation, In: *Applications of Mathematics in Technical and Natural Sciences, Sozopol (Bulgaria)*, *AIP Conference Proceedings*, **1301** (2010), 395.

[14] N. Kolkovska, K. Angelow, Numerical computation of the critical energy constant for two-dimensional Boussinesq equations, In: *Applications of Mathematics in Technical and Natural Sciences: 7th International Conference for Promoting the Application of Mathematics in Technical and Natural Scienses, Albena (Bulgaria)*, *AIP Conference Proceedings*, **1684** (2015), # 080007; https://doi.org/10.1063/1.4934318.

[15] P. Northrop, P.A. Ramachandran, W. Schiesser, V.R. Subramanian, A robust false transient method of lines for elliptic partial differential equations, *Chemical Engineering Science* **90** (2013), 3239.

[16] B. Fornberg, Generation of finite difference formulas on arbitrarily spaced grids, *Math. Comput.*, **51** (1988), 699-706.